Manuscript Draft: Aim3 Leaf Traits

Bolívar Aponte Rolón   Mareli Sánchez Juliá   A. Elizabeth Arnold
Sunshine A. Van Bael

2024-01-04

1 Abstract

2 Keywords:

Atta colombica, Calonectria, foliar fungal endophytes, herbivory, pathogen, tropical trees, symbioses

3 Introduction

Hypothesis 2 If FEF improves leaf defenses against plant pests, then generalist herbivores and pathogens will remove or damage less leaf tissue from plants with treated high FEF levels relative to those with low FEF loads.

Predictions.

Leaf-cutter ants will remove less plant material from leaves with higher FEF abundance and richness, but this result will be modulated by leaf traits related to defenses. Leaves with longer lifespans will be less attractive to leaf-cutter ants. Alternatively, low FEF diversity in those leaves may outweigh this selection factor. Leaves treated with high FEF levels will have a smaller area of pathogen damage compared to those treated with

low FEF levels. Endophyte-mediated defenses against pathogens will be most important in short-lived leaves

since long-lived leaves are expected to rely more on constitutive defenses (e.g., leaf toughness).

4 Materials and Methods

4.1 Field

Growth and host plant inoculation seven tropical tree species was conducted at the greenhouses in the Gamboa

Research Station, Smithsonian Tropical Research institute, Republic of Panama. The species, *Theobroma ca-*

cao, *Dypterix* sp., *Lacmellea panamensis*, *Apeiba membranacea*, *Heisteria concinna*, *Chrysophyllum caim-*

ito, and *Cordia alliodora* were chosen due to their variance in leaf traits (J.Wright unpublished data) and the

availability of seeds in January- April 2019. Seeds of tree species were collected from the forest floor and

grown in the greenhouse. Seedlings were kept in a chamber made out of PVC and clear plastic to prevent in-

oculation from spore fall inside the greenhouse. NEEDS INFORMATION ON THE SOIL MIXTURE AND

AUTOCLAVING PROTOCOL. Seedlings reached a minimum of 4 true leaves before endophyte inoculation.

Then 10 individual plants of each species were exposed to 10 nights of spore fall to achieve a high endophyte

load (E+) and 10 homologous plants were kept inside the greenhouse plastic chamber to maintain a low en-

dophyte load (*E*-) (Fig. ? MAKE A DIRAGRAM?). Plants exposed to spore fall were placed near (~10 m)

the forest edge at dusk (~18:OO hours) and returned to the greenhouse at dawn (~07:00 hours) (Bittleston et

al., 2011).

4.1.1 Leaf trait measurements

Three mature leaves were haphazardly collected from each of the individual plants in each treatment (E+,

E-) within 7-10 days after inoculation treatment. Anthocyanin (ACI) content and leaf thickness (LT) were

2

measured while the leaf was still attached to the plant. We measured anthocyanin content with ACM-200plus

(Opti-Sciences Inc. Hudson, New Hampshire, U.S.A.) on three haphazardly selected locations (working from

the petiole out to the leaf tip) on the leaf surface of three haphazardly selected leaves for a total of nine mea-

surements per plant (Tellez et al., 2022). The ACM-200 calculates an anthocyanin content index (ACI) value

from the ratio of % transmittance at 931 nm/% transmittance at 525 nm (**opti-sciencesinc?**) . On compound

leaves (i.e., *Dypterix* sp.) we measured at three different leaflets. Leaf thickness (μm) was measured with

a Mitutoyo 7327 Micrometer Gauge (Mitutoyo, Takatsu-ku, Kawasaki, Japan) in sthe same manner as the

anthocyanin measurements, taking care to avoid major and secondary veins. After anthocyanin and leaf thick-

ness measurements were completed, we removed the leaves from their stems, placed them inside a plastic bag

(i.e. Ziploc), place in an ice chest and moved them to the lab for further measurements. Leaf punch strength

(LPS) was measured with an Imada DST-11a digital force gauge (Imada Inc., Northbrook, IL, United States)

by conducting punch-and-die tests with a sharp-edged cylindrical steel punch (2.0 mm diameter) and a steel

die with a sharp-edged aperture of small clearance (0.05 mm). The leaf punch measurements were taken

by puncturing the leaf lamina at the base, mid-leaf and tip on both sides of the mid-vein, avoiding minor

leaf veins when possible (Tellez et al., 2022). Once leaf toughness was measured, we used a 7 mm diameter

punch hole to puncture disks for leaf mass per area (LMA) measurements. We collected one three disks per

leaf (see Supplementary material for details). The disk punches dried at 60 °C for 48-72 hours. before being

weighed.

4.1.2 Leaf tissue preparation for molecular work

The selected leaves were also used to profile endophyte community composition, abundance, and richness

via amplicon sequencing (Illumina MiSeq). The leaf tissue remaining after the leaf trait measurements had

the main vein and margins excised so that only the lamina remained. The lamina was haphazardly cut into 2

x 2 mm segments, enough to obtain a total of 16, and surface sterilized by sequential rinsing in 95% ethanol

(10 s), 0.5 NaOCl (2 mins) and 70% ethanol (2 mins), as per (Arnold et al., 2003; Higgins et al., 2014; Tellez et al., 2022). After, leaves were air-dried briefly under sterile conditions. Sixteen leaf segments per leaf, a total of forty-eight leaf segments per plant, were plated in 2% malt extract agar (MEA), sealed with Parafilm M (Bemis Company Inc., U.S.A.) and incubated at room temperature. The cultured leaf segments were used to estimate endophyte colonization of *E-* and *E+* leaves. The presence or absence of endophytic fungi in the leaf cuttings was assessed 7 days after plating. The remaining sterilized leaf lamina was preserved in sterile 15 mL tubes with ~ 10 mL CTAB solution (1 M Tris–HCl pH 8, 5 M NaCl, 0.5 M EDTA, and 20 g CTAB). Leaf tissue in CTAB solution was used for amplicon sequencing (described in detail below). All leaf tissue handling was performed in a biosafety cabinet with all surfaces sterilized by exposure to UV light for 30 minutes and cleaned sequentially in between samples with 95% ethanol, 0.5% NaOCl and 70% ethanol to prevent cross contamination.

4.2 Amplicon sequencing

Leaf tissue in CTAB solution was stored for 2 months at room temperature prior to being placed at -80 C for 3 months before extracting DNA. In preparation for DNA extraction, we decontaminated all instruments, materials, and surfaces with DNAway (Molecular BioProducts Inc., San Diego, CA, United States), 95% Ethanol, 0.5 % NaOCl, and 70 % Ethanol, and subsequently treated with UV light for 30 minutes in biosafety cabinet. We then transferred 0.2 – 0.3 g of leaf tissue into duplicate sterile 2mL tubes, resulting in 2 subsamples. Total genomic DNA from subsamples was extracted as described in U'Ren & Arnold (2017). In brief, we added two sterile 3.2 mm stainless steel beads to each tube and proceeded to lyophilize samples for 72 hours to fully remove CTAB content from tissue. After this period, we submerged the sample tubes in liquid nitrogen for 30s and proceeded to homogenize samples to a fine powder for 45 s in FastPrep-24 Tissue and Cell Homogenizer (MP Biomedicals, Solon, OH, USA). Afterwards, we repeated the decontamination procedure described before and used QIAGEN DNeasy 96 PowerPlant Pro-HTP Kit (U'Ren & Arnold, 2017)

4

(QIAGEN, Valencia, CA, USA). After all genomic DNA was extracted, we pooled the subsamples for each individual sample before amplification. We used sterile equipment and pipettes with aerosol-resistant tips with filters in all steps before amplification. We followed a two-step amplification approach previously described by Sarmiento et al. (2017) and U´Ren & Arnold (2017). We used primers for the fungal ITSrDNA region, ITS1f (5'-CTTGGTCATTTAGAGGAAGTAA-3') and ITS4 (5'-TCCTCCGCTTATTGATATGC-3') with modified universal consensus sequences CS1 and CS2 and 0–5 bp for phase-shifting. Every sample was amplified in two parallel reactions containing 1-2 µL of DNA template (U'Ren & Arnold, 2017; see also Tellez et al., 2022). We visualized PCR (PCR1) reactions with SYBR Green 1 (Invitrogen, Carlsbad, CA, USA) on 2% agarose gel (Oita et al., 2021). Based on the electrophoresis band intensity, we combined parallel PCR1 reactions and diluted 5 µL of amplicon product with molecular grade water to standardize to a concentration of 1:15 (Sarmiento et al., 2017 for details; Tellez et al., 2022). We included DNA extraction blanks and PCR1 negatives in this step. We used a separate set of sterile pipettes, tips, and equipment to reduce contamination. We used a designated PCR area to restrict contact with pre-PCR materials (Oita et al., 2021).

We used 1 µL of PCR1 product from samples and negative control for a second PCR (PCR2) with barcode adapters (IBEST Genomics Resource Core, Moscow, ID, USA). Each PCR2 reaction (total 15 µL) contained 1X Phusion Flash High Fidelity PCR Master Mix, 0.075 µM of barcoded primers (forward and reverse pooled at a concentration of 2 µM) and 0.24mg/mL of BSA following Sarmiento (2017) and U'Ren & Arnold (2017). Before final pooling for sequencing, we purified the amplicons using Agencourt AMPure XP Beads (Beckman Coulter Inc, Brea, CA USA) to a ratio of 1:1 following the manufacturer's instructions. The products were evaluated with Bio Analyzer 2100 (Agilent Technologies, Santa Clara, CA, USA) (Tellez et al., 2022). We quantified the samples through University of Arizona Genetics Core, and subsequently diluted them to the same concentration to prevent over representation of samples with higher concentration, see (CITATION). Amplicons were normalized to 1 ng/µL, then pooled 2 µL of each for sequencing. No contamination was

107 detected visually or by fluorometric analysis. To provide robust controls we combined 5 µL of each PCR1

108 negative and the DNA extraction blanks and sequenced them as samples. Ultimately, we combined samples

109 into a single tube with 20 ng/µL of amplified DNA with barcoded adapters for sequencing on the Illumina

110 MiSeq platform with Reagent Kit v3 (2 × 300 bp) following protocols from the IBEST Genomics Resource

111 Core at the University of Idaho, USA. Again, we included the DNA extraction blanks and two PCR1 negatives

112 and sequenced with samples. Sequencing yielded 3,778,081 total ITS1 reads.

4.2.1 Mock Communities

114 We processed and sequenced 12 mock communities following the methods described above. This allowed

115 us to assess the quality of our NGS data set. We used two mock communities that consisted of PCR product

116 from DNA extractions of 32 phylogenetically distinct fungi, representing lineages that are typically observed

117 as endophytes: Ascomycota, Basidiomycota, Zygomycota and Chytridiomycota (Oita et al., 2021; see Daru

118 et al., 2019 for details). In brief, we used six mock communities with equimolar concentrations of DNA

119 from all 32 fungal taxa and another six mock communities with tiered concentrations of DNA from the same

120 fungal taxa (Daru et al., 2019). Each mock community was sequenced five times (i.e., five replicates) (Oita

121 et al., 2021). The read abundance from the equimolar and tiered communities was positively associated with

122 the expected read number (with replicates as a random factor: R2Adj = 0.87, P = XXXX, see Supplementary

123 Material). Using mock communities allowed us to evaluate the sequencing effectiveness in communities

124 with known composition and structure (Bowman & Arnold, 2021). Henceforth, we used read abundance as

125 a relevant proxy for biological OTU abundance (U'Ren et al., 2019).

6

4.2.2 Bioinformatic analyses

We used VSEARCH (v2.14.1) for *de novo* chimera detection, dereplication and sequence alignment. VSEARCH is an open-source alternative to USEARCH that uses an optimal global aligner (full dynamic programming Needleman-Wunsch), resulting in more accurate alignments and sensitivity (Rognes et al., 2016). For mock communities and experimental samples, we used forward reads (ITS1) for downstream bioinformatics analyses due to their high quality, rather than reverse reads (ITS4). Following Sarmiento et al. (2017), we concatenated all reads in a single file and used FastQC reports to assess Phred scores above 30 and determine the adequate length of truncation. We processed 892,713 of sequence reads from mock communities and 3,778,081 from experimental samples. We truncated mock community and experimental sample reads to a length of 250 bp with command `fast_trunclen` and filtered them at a maximum expected error of 1.0 with command `fast_maxee`. We then clustered unique sequence zero radius OTUs (that is, zOTUs; analogous to amplicon sequence variants (Callahan et al., 2016)), by using commands `derep_fulllength` and `minseqlength` set at 2. Sequentially we denoised and removed chimeras from read sequences with commands `cluster_unoise`, and `uchime3_denovo`, respectively (see Supplementary YYY for details). Finally, we clustered zOTUs at a 95% sequence similarity with command `usearch_global` and option `id` set at 0.95. After which, 3,035,960 sequence reads from experimental samples remained.

Taxonomy was assigned with the Tree-Based Alignment Selector Toolkit [v2.2; Carbone et al. (2019)] by placing unknowns within the Pezizomycotina v2 reference tree (Carbone et al., 2017). ITS sequences were blasted against the UNITE database by the ribosomal database project (RDP) classifier. A total of 2147 OTUs hits were obtained and are composed of 68.6% Ascomycota, 26.8% Basidiomycota, <0.05% Chytridiomycota, <0.05% Glomeromycota, <0.05% Mortierellomycota, <0.05% Rozellomycota, 0.05% Kickxellomycota, and 4.2 % BLAST hit misses. Only OTUs representing Ascomycota were used for downstream statistical analy-

ses since foliar endophyte communities in tropical trees are dominated by Ascomycota (Arnold & Lutzoni, 2007).

For each OTU identified, we removed laboratory contaminants from experimental samples by substracting the average read count found in control samples from the DNA extraction and PCR steps. Our analysis of mock communities allowed use to identify and remove false OTUs from experimental samples, those with fewer than 10 reads, and remove 0.1% of the read relative abundance across all samples (Oita et al., 2021). Removed reads represent the frequency of reads classified as contamination in the mock communities relative to the expected read count. Three experimental samples from *Theobroma cacao* (n=2) and *Apeiba membranacea* (n=1) were removed from all analyses due to incomplete entries. After pruning taxa with zero reads from experimental samples, we identified 260 OTUs found exclusively in control ($E-$) plants (n=78) and deemed them as artifacts resulting from the greenhouse conditions. Consequently, these were consistently eliminated from treatment ($E+$) plants across all species. We converted reads for each fungal OTU to proportions of total sequence abundance per sample to reduce differences in sampling effort, following previous studies (Weiss et al. (2017); McMurdie & Holmes (2014)). We then removed singletons and obtained an average of 2,464,558 sequence reads in 529 Ascomycota OTUs across 156 experimental samples of 7 tree species. All analyses post taxonomic assignment were performed in R [v. 4.3.2; R Core Team (2023)] using the `phyloseq` package (McMurdie & Holmes, 2013) and custom scripts (see Supplementary Material).

4.2.3 Ant-endophyte interaction assays

A fresh fourth leaf was used in ant assays. To assess leaf-cutter ant damage, we introduced one detached leaf per plant per treatment to an actively foraging leaf-cutter ant colony for a two-hour assay. We presented leaf-cutter ant colonies with a choice of an E+ or an E- leaf on one disposable plastic plate next to an active nest trail. Carefully, we collected and placed debris from the trail leading up to the plate to lure ants into

the plate. We initiated the ant assay as soon as one ant entered the plate and explored the leaf contents (for

~ 10-20 seconds). Every five minutes we took a digital photo of the choice arena until about 75% of the

leaf content of one of the leaves was consumed. We used the digital photo at time zero and at the end of

trial to quantify the leaf area removed using ImageJ [v1.52r; Schneider et al. (2012)]. Ant recruitment was

estimated by counting individuals in the choice arena throughout trial event.

4.2.4 Pathogen assays

For the pathogen assays, we introduced an agar plug inoculated with hyphae of *Calonectria* sp. ($P+$ treat-

ment), and an agar plug without the pathogen ($P-$ control) to similarly aged/sized leaves within 10-14 days

after endophyte inoculations (CITATION). Leaves with the $P+$ or $P-$ treatment were misted with sterile

water two times a day (morning and afternoon) to maintain moisture. After four days, we removed the plugs

and took digital photos to analyze leaf area damage using ImageJ [v1.52r; Schneider et al. (2012)].

4.2.5 Replication Statement (maybe goes before statistical analyses)

*In the Materials and Methods section (before the description of the data analyses), authors **MUST** state i) the*

scale at which they seek to make inferences (for example at the level of species, populations or experimental

units); ii) the scale(s) at which their treatment or factor of interest is(are) applied; and iii) the number

of replicates for each level of treatment or factor. We have provided a table template for including this

information, which the editors will use to decide whether the authors' inferences are supported and should

therefore be peer-reviewed. Manuscripts without this table will be returned to authors.

4.2.6 Statistical Analyses

We explored how leaf functional traits and foliar fungal symbionts correlated to herbivory and pathogen damage on leaves. We present the analyses at the leaf and at the plant level. Leaf functional traits were measured and are presented in their raw form, at the leaf level, while FEF data was explored and is presented at the plant level. In analyses where leaf functional traits and FEF are combined we used averages of the leaf functional traits.

Principal Component Analysis (PCA) was used to reduce dimensions among covariates and reveal underlying interactions that could influence fungal endophyte abundance, diversity and community composition in seedlings. The PCA was computed using the `prcomp` function in R statistical software (R Core Team, 2023). A complete PCA was computed with variables ACI, LT, LPS, and LMA (Fig. 2a). We then proceeded to compute a PCA with the data from leaves of plants used in the ant ($n = 210$) and pathogen assays ($n = 192$). To further explore the interactions of herbivory and pathogen damage ACI, LT, LPS and LMA we computed simple linear regressions (Fig. S6 - S7).

To test for H2, we used a general linear mixed model (GLM) with herbivory and pathogen damage percentage (logit transformed) as the response variable. To determine which fixed effects to include in the models we used the `vif` function in *R* to calculate the variance inflation factor for all explanatory variables (ACI, LT, LPS and LMA) (R Core Team, 2023). We then created a correlation matrix with `cor` function to assess correlations among covariates (SUPPLEMENTARY FIGURE?). We opted to maintain explanatory variables pertaining to physical barriers (LT, LPS and LMA) and exclude ACI from subsequent general linear models due to high collinearity with LPS ($r = 0.54$) and LMA ($r = 0.73$). Every variable kept exhibits some degree of collinearity and this is well recorded in the literature (CITE HERE).

5 Results

Seedlings exposed to forest spore fall, *E+*, had a significantly higher proportion of leaf segments colonized by fungal endophytes across all species (data from cultures, Fig. S1) Using our molecular data set we saw that seedlings with *E+* treatment had a significantly higher fungal endophyte relative abundance (p <0.05) for all tree species when compared to *E-* treatment with the exception of *C. cainito* and *H. concinna* (Fig. 1). Despite these significant differences, there is a high degree of variability in endophyte relative abundance within each treatment type (Fig. 1).

For individuals of all tree species, we observed general differences in leaf functional traits summarized in Table 1. For LT we observed significant differences for *A. membranacea* , *Dypteryx* sp., and *L. panamensis* despite treatment type. Anthocyanins (ACI) were all leaf functional traits across all tree species. We did not see (CONTINUE HERE)

THE PARAGRAPH ABOVE NEEDS A LOT OF WORK. I NEED THE PLOTS FOR THIS TO WRITE ABOUT IT.

The PCA revealed how leaf traits (ACI, LT, LPS and LMA) were related. We plotted leaf trait data according to tree species groups on the PCA axes to show how the variance in the complete data set is explained by PC1 (60%) and PC2 (27%) (Fig. 2a). We observed that ACI, LPS and LMA loadings tracked along PC1 towards more negative values, showing correlation among these traits (Fig. 2a). Traits LT and LPS were orthogonal to each other in Fig. 2a, indicative of low correlation. We note distinct grouping of species along PC1 such as *C. alliodora* in the direction of positive values of PC1 and *C. cainito* towards negative values. Along PC1 we see distinct and tight clustering according to species for all except *H. concinna* and *A. membranacea* which overlap with various other species. We note that LT loading tracks towards negative values along PC2 (Fig.2a). Clear species groupings are detected, such as *Dypterix* sp. located towards positive values and *L. panamensis* towards negative values of the PC2 axis. We note a similar relationship between the leaf traits

11

with respect to PC1 and PC2 in individual seedlings used for herbivory versus pathogen damage trials (Fig. 2b-2c). The PCA of leaf traits from seedlings used in herbivory trials has a PC1 explaining 57.5% of the variance and a PC2 explaining 28% of the variance in the subset data (Fig. 2b). We saw an inversion of the LT loading in direction of positive values, as well as the main tree species clustered (i.e. *Dypteryx* sp. and *A. membranacea*) along PC2 (Fig. 2b) with respect to Fig. 2a. The PCA of leaf traits from seedling used in pathogen damage trials has a PC1 explaining 64% of the variance and a PC2 explaining 25% of the variance in the subset data (Fig. 2c). We detected similar relationships among leaf traits and PC axes in the pathogen damage subset data (Fig. 2c) when compared to the complete data set (Fig. 2a).

Simple linear regressions of herbivory (%) against PC1 and PC2 revealed a statistically significant positive relationship (p <0.001) (Fig. 3a and 3b). Even though we note large spread in the data (Fig. 3a and 3b), we see a statistically significant positive trend of herbivory plotted against PC1, where positive values represent greater values of ACI, LPS and LMA. Herbivory plotted against PC2 shows a statistically significant positive trend, where positive values represent greater LT (Fig. 3b). Percent pathogen damage plotted against PC1 revealed a statistically significant positive relationship (p = <0.001), in which positive values represent greater values of ACI, LPS and LMA (Fig. 3c). We did not see a statistically significant relationship (p = 0.223) between pathogen damage and PC2 (Fig. 3d).

TALK ABOUT SIMPLE LINEAR REGRESSIONS OF SUPPLEMENTARY FIGURES?

6 Discussion

7 References

Arnold, A. E., & Lutzoni, F. (2007). Diversity and host range of foliar fungal endophytes: Are tropical leaves biodiversity hotspots? *Ecology*, *88*(3), 541–549. https://doi.org/10.1890/05-1459

Arnold, A. E., Mejía, L. C., Kyllo, D., Rojas, E. I., Maynard, Z., Robbins, N., & Herre, E. A. (2003). Fungal endophytes limit pathogen damage in a tropical tree. *Proceedings of the National Academy of Sciences*, *100*(26), 15649–15654.

Bittleston, L. S., Brockmann, F., Wcislo, W., & Van Bael, S. A. (2011). Endophytic fungi reduce leaf-cutting ant damage to seedlings. *Biology Letters*, *7*(1), 30–32. https://doi.org/10.1098/rsbl.2010.0456

Bowman, E. A., & Arnold, A. E. (2021). Drivers and implications of distance decay differ for ectomycorrhizal and foliar endophytic fungi across an anciently fragmented landscape. *The ISME Journal*, *15*(12), 3437–3454. https://doi.org/10.1038/s41396-021-01006-9

Callahan, B. J., McMurdie, P. J., Rosen, M. J., Han, A. W., Johnson, A. J. A., & Holmes, S. P. (2016). DADA2: High-resolution sample inference from Illumina amplicon data. *Nature Methods*, *13*(7), 581–583. https://doi.org/10.1038/nmeth.3869

Carbone, I., White, J. B., Miadlikowska, J., Arnold, A. E., Miller, M. A., Kauff, F., U'Ren, J. M., May, G., & Lutzoni, F. (2017). T-BAS: Tree-Based Alignment Selector toolkit for phylogenetic-based placement, alignment downloads and metadata visualization: An example with the Pezizomycotina tree of life. *Bioinformatics*, *33*(8), 1160–1168. https://doi.org/10.1093/bioinformatics/btw808

Carbone, I., White, J. B., Miadlikowska, J., Arnold, A. E., Miller, M. A., Magain, N., U'Ren, J. M., & Lutzoni, F. (2019). T-BAS Version 2.1: Tree-Based Alignment Selector Toolkit for Evolutionary Placement of DNA Sequences and Viewing Alignments and Specimen Metadata on Curated and Custom Trees. *Microbiology Resource Announcements*, *8*(29), e00328–19. https://doi.org/10.1128/MRA.00328-19

Daru, B. H., Bowman, E. A., Pfister, D. H., & Arnold, A. E. (2019). A novel proof of concept for capturing the diversity of endophytic fungi preserved in herbarium specimens. *Philosophical Transactions of the Royal Society B: Biological Sciences*, *374*(1763), 20170395. https://doi.org/10.1098/rstb.2017.0395

Higgins, K. L., Arnold, A. E., Coley, P. D., & Kursar, T. A. (2014). Communities of fungal endophytes in tropical forest grasses: Highly diverse host- and habitat generalists characterized by strong spatial

structure. *Fungal Ecology*, *8*(1), 1–11. https://doi.org/10.1016/j.funeco.2013.12.005

McMurdie, P. J., & Holmes, S. (2013). Phyloseq: An R Package for Reproducible Interactive Analysis and Graphics of Microbiome Census Data. *PLoS ONE*, *8*(4), e61217. https://doi.org/10.1371/journal.pone.0061217

McMurdie, P. J., & Holmes, S. (2014). Waste Not, Want Not: Why Rarefying Microbiome Data Is Inadmissible. *PLoS Computational Biology*, *10*(4), e1003531. https://doi.org/10.1371/journal.pcbi.1003531

Oita, S., Ibáñez, A., Lutzoni, F., Miadlikowska, J., Geml, J., Lewis, L. A., Hom, E. F. Y., Carbone, I., U'Ren, J. M., & Arnold, A. E. (2021). Climate and seasonality drive the richness and composition of tropical fungal endophytes at a landscape scale. *Communications Biology*, *4*(1), 313. https://doi.org/10.1038/s42003-021-01826-7

R Core Team. (2023). *R: A Language and Environment for Statistical Computing* [Computer software]. R Foundation for Statistical Computing. https://www.R-project.org/

Rognes, T., Flouri, T., Nichols, B., Quince, C., & Mahé, F. (2016). VSEARCH: A versatile open source tool for metagenomics. *PeerJ*, *4*, e2584. https://doi.org/10.7717/peerj.2584

Sarmiento, C., Zalamea, P. C., Dalling, J. W., Davis, A. S., Simon, S. M., U'Ren, J. M., & Arnold, A. E. (2017). Soilborne fungi have host affinity and host-specific effects on seed germination and survival in a lowland tropical forest. *Proceedings of the National Academy of Sciences of the United States of America*, *114*(43), 11458–11463. https://doi.org/10.1073/pnas.1706324114

Schneider, C. A., Rasband, W. S., & Eliceiri, K. W. (2012). NIH Image to ImageJ: 25 years of image analysis. *Nature Methods*, *9*(7), 671–675. https://doi.org/10.1038/nmeth.2089

Tellez, P. H., Arnold, A. E., Leo, A. B., Kitajima, K., & Van Bael, S. A. (2022). Traits along the leaf economics spectrum are associated with communities of foliar endophytic symbionts. *Frontiers in Microbiology*, *13*, 927780. https://doi.org/10.3389/fmicb.2022.927780

Tellez, P. H., Rojas, E., & Van Bael, S. (2016). Red coloration in young tropical leaves associated with

302 reduced fungal pathogen damage. *Biotropica*, *48*(2), 150–153. https://doi.org/10.1111/btp.12303

303 U'Ren, J. M., & Arnold, A. E. (2017). 96 well DNA Extraction Protocol for Plant and Lichen Tissue Stored

304 in CTAB. *Protocols.io*, 1–5.

305 U'Ren, J. M., Lutzoni, F., Miadlikowska, J., Zimmerman, N. B., Carbone, I., May, G., & Arnold, A. E.

306 (2019). Host availability drives distributions of fungal endophytes in the imperilled boreal realm. *Nature*

307 *Ecology & Evolution*, *3*(10), 1430–1437. https://doi.org/10.1038/s41559-019-0975-2

308 Weiss, S., Xu, Z. Z., Peddada, S., Amir, A., Bittinger, K., Gonzalez, A., Lozupone, C., Zaneveld, J. R.,

309 Vázquez-Baeza, Y., Birmingham, A., Hyde, E. R., & Knight, R. (2017). Normalization and microbial

310 differential abundance strategies depend upon data characteristics. *Microbiome*, *5*(1), 27. https://doi.org/

311 10.1186/s40168-017-0237-y

8 Figures

8.1 Figure 1

8.2 Figure 2

8.3 Figure 3

8.4 Figure 4

317 Linear mixed effects models for predicting leaf herbivory and pathogenicity
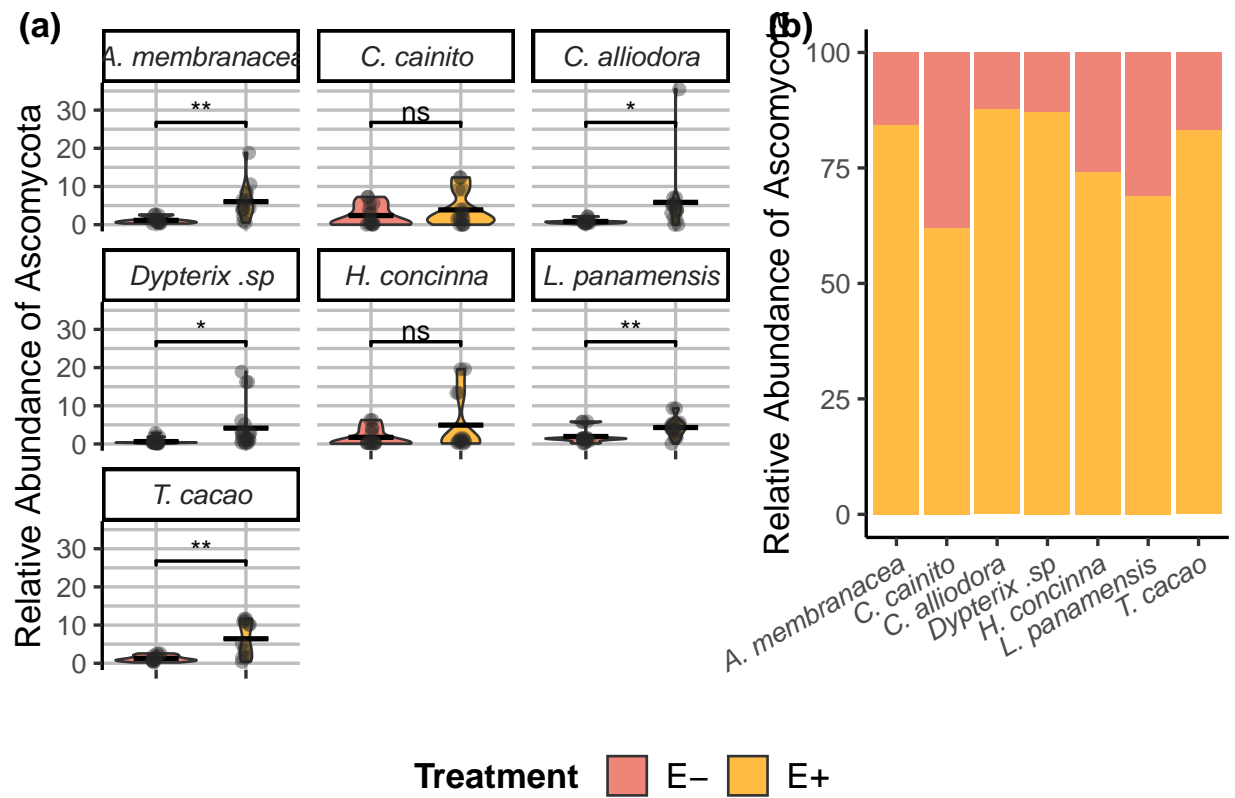
318

319 logit herbivory

320 logit pathogenicity

Figure 1: Relative abundance (RA) of Ascomycota OTUs of seven tree species used in the study. (a) Violin plots show individuals' RA and and its distribution by species. The horizontal line within the violins represent the mean RA per species. (b) The RA of OTU's by treatment withing each tree species. Pink filled violin plots represent low endophyte (*E-*) treatment and yellow filled represent high endophyte (*E+*) treatment. Relative abundance is the percentage of endophyte colonization within individuals of the same species. Significance levels are represented by asterisks [$p = 0.05$ (*), $p = 0.01$ (*)*, and* p* = 0.001 (***)].
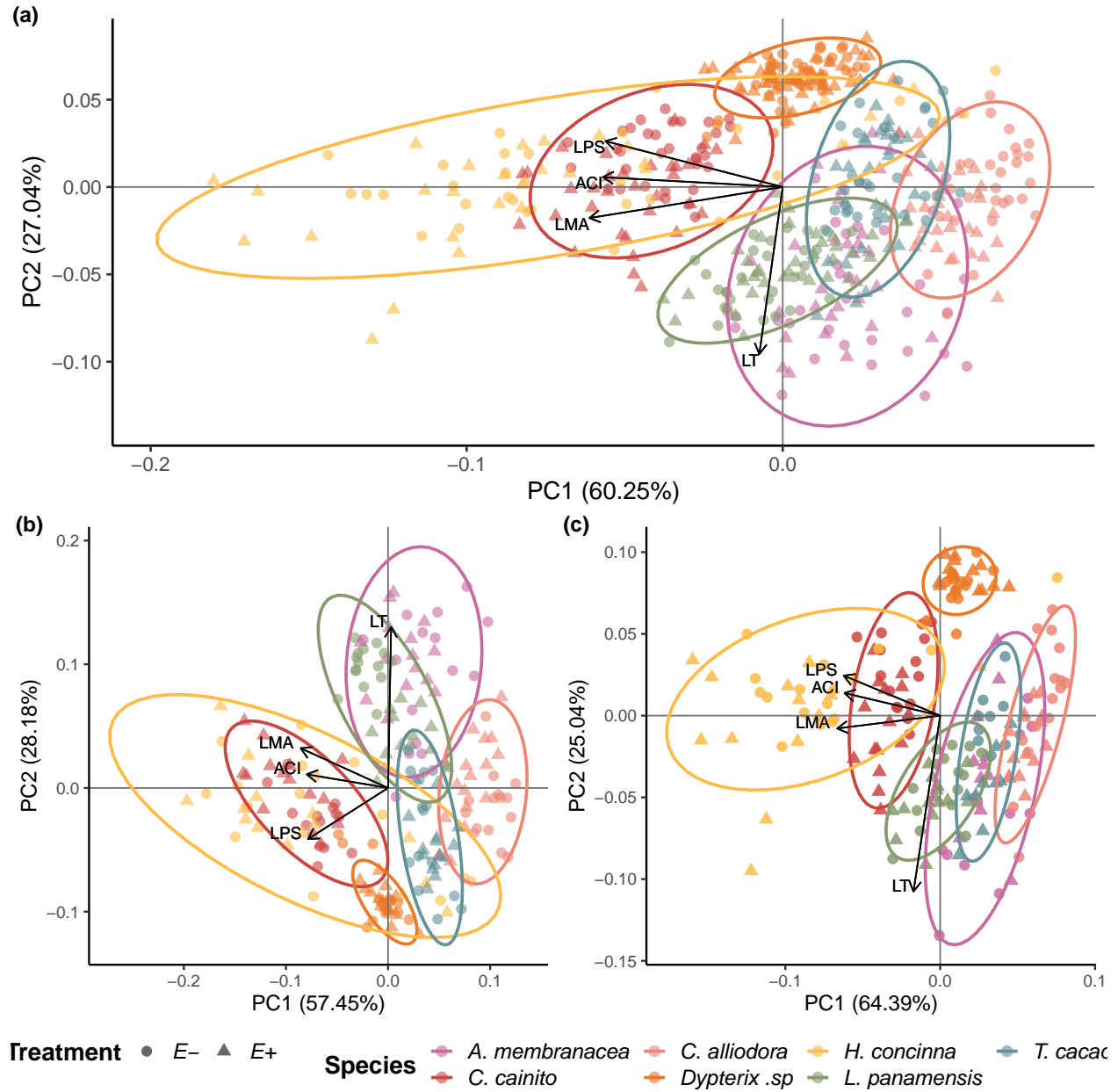
Figure 2: Leaf functional traits are conserved within tree species regardless of endophyte load treatment. (a) Principal Component Analysis (PCA) of leaf functional traits from all tree species separated by *E-* and *E+* treatment. (b) PCA of leaf functional traits of plants solely used in ant herbivory assays. (c) PCA leaf functional traits of plants used solely in pathogen damage assays. Colors represent individual species. Circle and triangles represent low (*E-*) and high (*E+*) endophyte treatments, respectively. Colored ellipses correspond to tree species and represent 95% confidence intervals.
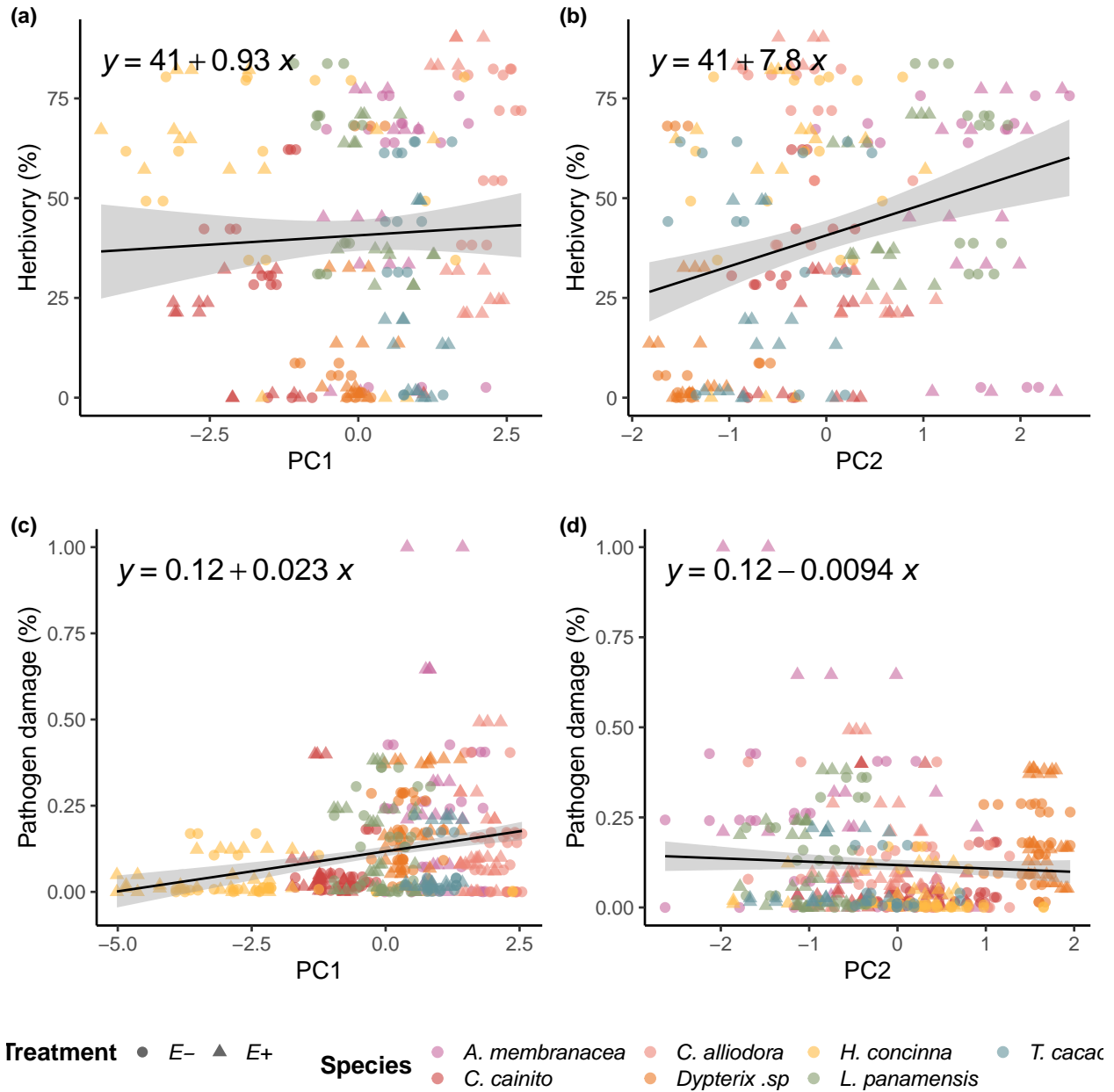
Figure 3: Simple linear regressions of herbivory and pathogen damage on PC1 and PC2 axes from PCAs of leaf traits for ant herbivory and pathogen damage assays. Linear regression of a) percent herbivory damage and PC1 axis (R^2-adjusted= -0.0024, p = 0.447); b) percent herbivory damage and PC2 axis (R^2-adjusted = 0.079, p = <0.001); c) percent pathogen damage and PC1 axis (R^2-adjusted = 0.064, p = <0.001); and d) percent pathogen damage and PC2 axis (R^2-adjusted = 0.0016, p = 0.207). Colors represent individual species. Circle and triangles represent E- and E+ treatments, respectively.

Predictors	Estimates	CI	p	Estimates	CI	p
(Intercept)	-0.26	-2.31 – 1.80	0.806	-3.42	-4.40 – -2.43	**<0.001**
Thickness	-0.01	-0.02 – -0.00	**0.013**	0.00		

340 -0.00 – 0.01

341 0.097

342 LMA

343 1741.22

344 768.82 – 2713.62

345 **0.001**

346 171.65

347 -181.40 – 524.70

348 0.340

349 E load [E+]

350 -0.78

351 -1.11 – -0.45

352 **<0.001**

353 Random Effects

354 σ^2

355 3.34

356 2.16

357 τ_{00}

358 1.93 $_{Species}$

359   0.80 $_{\text{Treatment}}$

360

361   0.02 $_{\text{E\_load}}$

362

363   0.96 $_{\text{Species}}$

364   ICC

365   0.37

366

367   N

368   7 $_{\text{Species}}$

369   2 $_{\text{Treatment}}$

370

371   2 $_{\text{E\_load}}$

372

373   7 $_{\text{Species}}$

374   Observations

375   210

376   382

377   Marginal R^2 / Conditional R^2

378   0.089 / 0.423

379   0.011 / NA

380   AIC

381   745.559

382   1012.259

383 8.5 Table 1

Table 1: Replication statement of the statistical analysis in this study.

Scale of inference	Scale at which the factor of interest is applied	Number of replicates at the appropriate scale

Leaf functional traits	Species	Treatment = 2 (E-, E+), Tropical tree species = 7. Replicates per species = 5. Replicate leaves per plant = 3
Genomic data	Species	Treatment = 2 (E-, E+), Replicates per species = 5
Herbivore and Pathogen trials	Species/individual	Treatment = 2 (E-, E+), Replicates per species = 5, Replicates per plant = 1

384 ## 8.6 Table 2

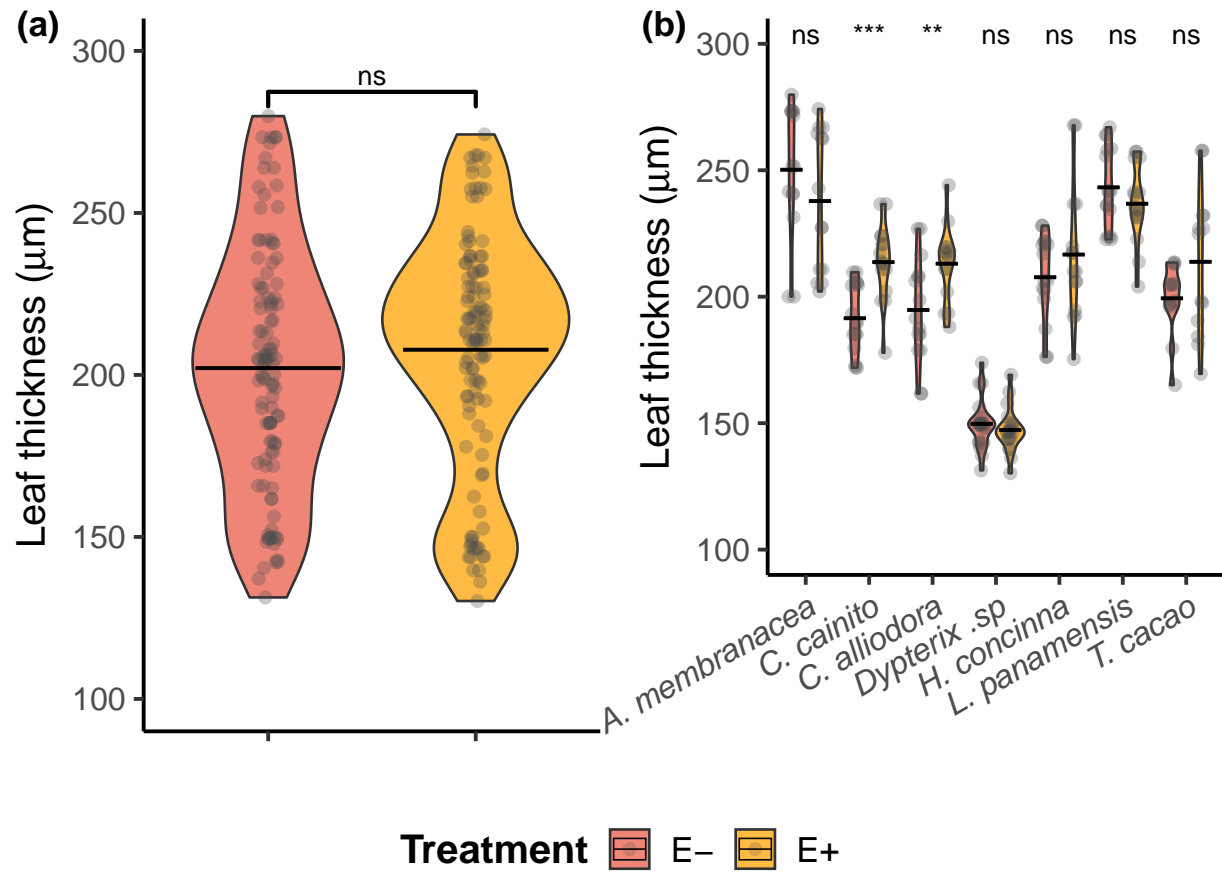|	*A. membranacea, n = 83[1]*	*C. alliodora, n = 100[1]*	*C. cainito, n = 150[1]*
Treatment			
E- (n = 570)	47	54	75
E+ (n = 544)	36	46	75
Anthocyanins (ACI)	5.35 ± 1.06	3.47 ± 0.43	8.21 ± 1.41
Leaf Thickness (LT) (μm)	270 ± 45	207 ± 37	205 ± 30
Leaf Punch Strength (LPS) (N mm/1)	0.22 ± 0.05	0.21 ± 0.05	0.53 ± 0.09
Leaf Mass per Area (LMA) (mg/mm)	0.0011 ± 0.0002	0.0007 ± 0.0001	0.0015 ± 0.0002

Figure 4: Figure S2: (a) Comparison of leaf thickness (LT) between *E-* and *E+* treatment groups. (b) Comparison of LT *E-* and *E+* treatment groups per species. Significance levels are represented by asterisks [*p* = 0.05 (*), *p* = 0.01 (*), and p* = 0.001 (***)].

9 Supplementary Materials

9.1 Figure S1

9.2 Figure S2a-S2b

Figure S2: (a) Comparison of leaf thickness (LT) between *E-* and *E+* treatment groups. (b) Comparison of LT *E-* and *E+* treatment groups per species. Significance levels are represented by asterisks [$p = 0.05$ (*), $p = 0.01$ (*), and p* = 0.001 (***)].
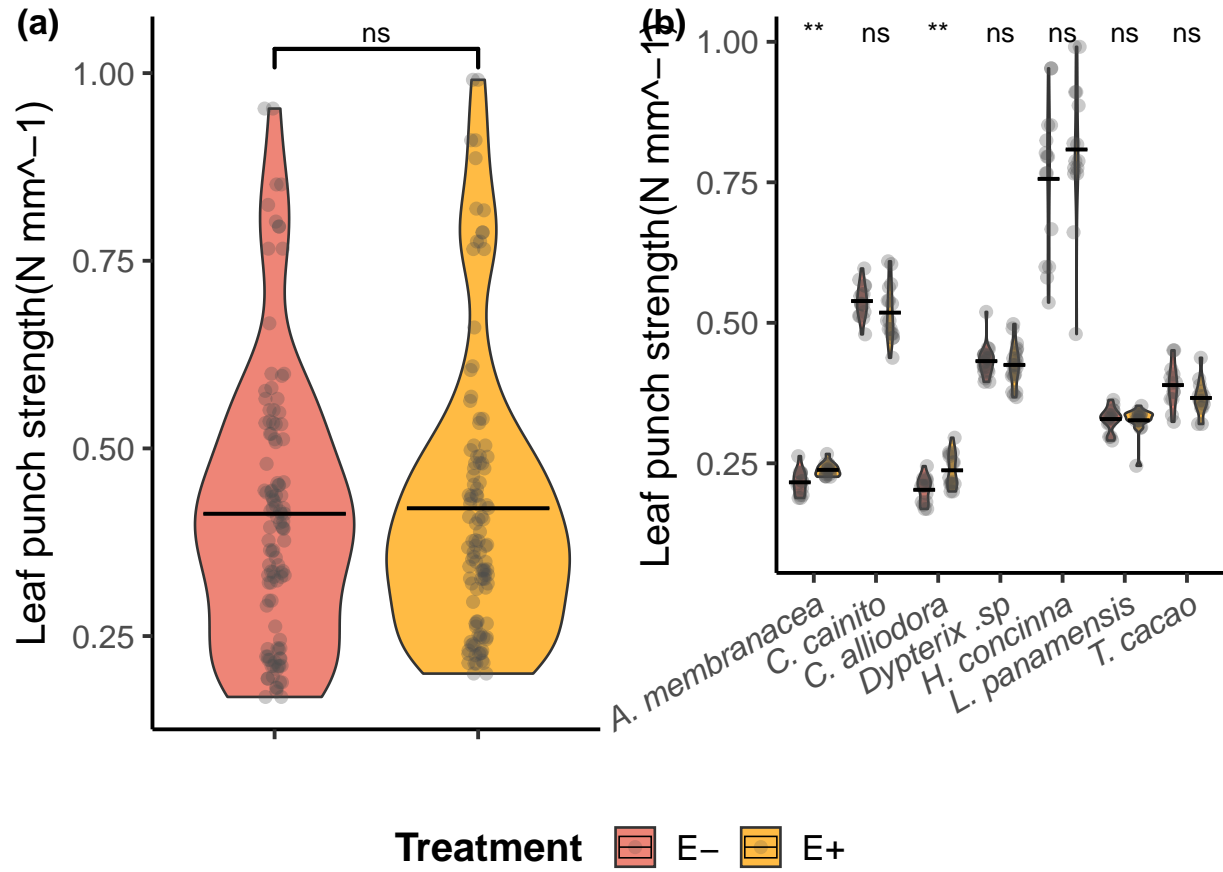
9.3 Figure S3a-S3b

Figure 5: Figure S2: (a) Comparison of leaf punch strength (LPS) between *E-* and *E+* treatment groups. (b) Comparison of LPS between *E-* and *E+* treatment groups per species. Significance levels are represented by asterisks [$p = 0.05$ (*), $p = 0.01$ (*), *and* p* = 0.001 (***)].

.y.	group1	group2	p	p.adj	p.format	p.signif	method
Thickness	APEIME	CHRYCA	1.79e-08	2.3e-07	1.8e-08	****	T-test
Thickness	APEIME	CORDAL	6.86e-08	8.2e-07	6.9e-08	****	T-test
Thickness	APEIME	DYPTE	7.84e-18	1.5e-16	< 2e-16	****	T-test
Thickness	APEIME	HEISCO	1.26e-05	0.0001	1.3e-05	****	T-test
Thickness	APEIME	LACPA	0.499	1	0.499	ns	T-test
Thickness	APEIME	THEOCA	1.6e-06	1.4e-05	1.6e-06	****	T-test
Thickness	CHRYCA	CORDAL	0.785	1	0.785	ns	T-test
Thickness	CHRYCA	DYPTE	2.6e-19	5.2e-18	< 2e-16	****	T-test
Thickness	CHRYCA	HEISCO	0.0688	0.48	0.069	ns	T-test
Thickness	CHRYCA	LACPA	1.38e-12	2.1e-11	1.4e-12	****	T-test
Thickness	CHRYCA	THEOCA	0.477	1	0.477	ns	T-test
Thickness	CORDAL	DYPTE	8.66e-17	1.5e-15	< 2e-16	****	T-test
Thickness	CORDAL	HEISCO	0.135	0.81	0.135	ns	T-test
Thickness	CORDAL	LACPA	1.16e-10	1.6e-09	1.2e-10	****	T-test
Thickness	CORDAL	THEOCA	0.648	1	0.648	ns	T-test
Thickness	DYPTE	HEISCO	8.18e-17	1.5e-15	< 2e-16	****	T-test
Thickness	DYPTE	LACPA	8.01e-32	1.7e-30	< 2e-16	****	T-test
Thickness	DYPTE	THEOCA	4.64e-13	7.4e-12	4.6e-13	****	T-test
Thickness	HEISCO	LACPA	7.27e-07	7.3e-06	7.3e-07	****	T-test
Thickness	HEISCO	THEOCA	0.365	1	0.365	ns	T-test
Thickness	LACPA	THEOCA	1.71e-07	1.9e-06	1.7e-07	****	T-test